Polarization of lines emitted after electron capture into $Ar^{7+}(nlm_l)$ sublevels during 80-keV Ar^{8+}-Li collisions

C. Laulhé,[1] E. Jacquet,[1,2] G. Cremer,[1,2] J. Pascale,[3] P. Boduch,[1,2] G. Rieger,[1,2] D. Lecler,[1] M. Chantepie,[1,2] and J. L. Cojan[1,2]

[1]*Laboratoire de Spectroscopie Atomique, CNRS-ERS 137, ISMRA, Bd Maréchal Juin, 14 050 Caen Cédex, France*

[2]*UFR des Sciences, Université de Caen, Esplanade de la Paix, 14032 Caen Cédex, France*

[3]*Service des Photons, Atomes et Molécules, Centre d'Etudes de Saclay CEA, Bâtiment 522, 91191 Gif sur Yvette Cédex, France*

(Received 12 May 1995; revised manuscript received 22 June 1995)

We have measured the polarization rates of lines emitted after single-electron capture occurring during Ar^{8+}-Li collisions at an impact energy of 80 keV. In order to obtain information on the final m_l values which are populated in the electron-capture process, we have also calculated the polarization rates from the nlm_l distributions determined by using the classical trajectory Monte Carlo (CTMC) method. The good agreement which is obtained between the experimental and the calculated polarization rates indicates the reliability of the CTMC method which predicts that $m_l=0$, ± 1, and ± 2 are preferentially populated by the electron-capture process.

PACS number(s): 34.50.−s

I. INTRODUCTION

Recent studies of Ar^{8+}-Li($2s$) collisions [1,2] at low or intermediate velocities ($v \leq 1$ a.u.), both experimentally by photon spectroscopy and theoretically by using the three-body classical trajectory Monte Carlo (CTMC) method [3,4] have shown that the single-electron-capture process populates $Ar^{7+}(nl)$ sublevels mainly with $n=8$ and 9. It was also found that sublevels with large angular momenta ($l \geq 5$) and, to a lesser extent, sublevels of low angular momenta ($l \leq 2$), are preferentially populated whereas sublevels of intermediate l values ($l=3$, 4) are almost not populated. The experimental and theoretical results were found to be in fair agreement.

These nonstatistical nl distributions are explained [2,5], from a phenomenological point of view, as due to a redistribution of the initial population involving two mechanisms: the Stark effect [6] due to the electric field of the residual Li^+ ion and the projectile core electron effect [7]. Explicitly, the Stark effect is mainly responsible for the population of final states with $l>3$ while the projectile core effect is seen in the population of final states with $l<3$.

According to Stark mixing calculations made by Salin [8] in the case of low velocity collisions between bare ions and hydrogen atoms, the nl distributions are a consequence of the Zeeman m_l sublevel distributions. It is shown that the produced states are characterized by *a strong alignment, with* $m_l=0$, ± 1 *predominantly populated* as a consequence of the primary capture process itself. In this sense, the final magnetic substate alignment is more representative of the collision than the nl distributions. Similar nonstatistical m_l distributions have been determined recently [9,10] from CTMC calculations for electron-capture collisions between multiply charged ions and ground-state alkali-metal atoms. In particular, for collisions between Ar^{8+} or Kr^{8+} ions with Li($2s$), it has been shown that the projectile electron core influences also the m_l distribution as the projectile energy decreases [10]. Efforts to measure magnetic sublevel distributions are then justified.

As a consequence of the nonstatistical Zeeman sublevel distributions, the radiative transitions, subsequent to the decay of the projectile excited states produced during the single-electron transfer, are expected to be polarized. Many experimental studies have already been presented. Most of them were devoted to polarization measurements of strong resonance lines emitted either in the x-ray or vuv range [11–14]. In the near uv range let us note the work of Roncin *et al.* [15] and in the visible range the work of Lembo *et al.* [16], who performed polarization rate measurements of Rydberg transitions following electron capture of Ne^{q+} ions on sodium atoms.

In order to measure the polarization rates of each line emitted between 200 and 600 nm and resulting from single-electron capture following 80-keV Ar^{8+}-Li($2s$) collisions, we have used an optical device composed of a polarimeter and a spectrometer. The method usually used to measure polarization rates in the visible wavelength range, i.e., using a specific filter for each emission line [16], was not fitted to our case. The final aim of our investigations was to estimate the degree of alignment of the produced states.

Since the experimental setup described in [1] was appropriate to detect these emissions, it was of interest to modify the detection device in order to perform accurate measurements of their polarization rates. In the present paper, we will describe in detail the modifications we introduced in the experimental setup. The results of the measurements will be compared with the results determined from CTMC calculations providing final nlm_l distributions.

II. EXPERIMENTAL SETUP

Beside the optical device needed for polarization measurements, the experimental setup is similar to that described in Ref. [1].

The Ar^{8+} ion beam was produced by an electron cyclotron resonance (ECR) ion source of the Grand Accélérateur National d'Ions Lourds, Caen, France (GANIL) test bench, with a beam current of nearly 100 μA. The incident ion

beam was focused on an effusive jet of lithium atoms produced by an oven heated to about 600 °C centered inside a collision chamber. The jet pressure was estimated to be about 1 mm Hg, while the pressure inside the collision chamber was maintained at 5×10^{-7} mbar.

The emitted light was detected at right angles to the directions of the incident ion beam and that of the lithium jet. After passing through a polarimeter, it was focused on the entrance slit of a normal incidence grating spectrometer of 700 mm focal length (Sopra 700) equipped with a 1200 grooves/mm grating blazed at 750 nm in the first order. The analyzed light was detected by a photomultiplier (HAMAMATSU R106) the signal of which was recorded on a tracing table.

The polarimeter is composed of two polarizers. The first one is a dichroic polarizer (Polacoat), and its polarization direction can be oriented parallel or perpendicular to the direction of the incident ion beam. The second one, placed in front of the entrance slit of the spectrometer, is a Glan-Taylor prism whose polarization direction is fixed at 45° to the ion beam direction.

The dichroic polarizer can be considered as a nonperfect polarizer with a principal transmission coefficient k_1 and a second transmission coefficient k_2 in the direction perpendicular to the principal one, whereas the Glan-Taylor prism can be considered as a perfect polarizer.

For the parallel orientation of the dichroic polarizer, the measured intensity is

$$i_{\parallel}=\alpha(k_1 I_{\parallel}+k_2 I_{\perp})\cos^2 45^\circ\cos^2(\theta-45^\circ), \tag{1}$$

where $I_{\parallel}$ and $I_{\perp}$ are the intensities of the emitted light polarized along and perpendicular to the ion beam direction respectively; α represents the detection efficiency; θ is the polarization angle of the grating. For the perpendicular orientation, the measured intensity is

$$i_{\perp}=\alpha(k_1 I_{\perp}+k_2 I_{\parallel})\cos^2 45^\circ\cos^2(\theta-45^\circ). \tag{2}$$

Let us denote $i_{\min}$ as the origin of the intensities, corresponding to the crossed position of both polarizers. $i_{\min}$ can be expressed as

$$i_{\min}=\alpha k_2(I_{\parallel}+I_{\perp})\cos^2 45^\circ\cos^2(\theta-45^\circ). \tag{3}$$

The maximum of the transmitted intensity, denoted $i_{\max}$, is obviously measured when both polarizers are parallel. The polarization rate defined by $\Gamma=(I_{\parallel}-I_{\perp})/(I_{\parallel}+I_{\perp})$ is then obtained by the relation

$$\Gamma=\frac{(i_{\parallel}-i_{\min})-(i_{\perp}-i_{\min})}{(i_{\parallel}-i_{\min})+(i_{\perp}-i_{\min})}=\frac{i_{\parallel}-i_{\perp}}{i_{\parallel}+i_{\perp}-2i_{\min}}. \tag{4}$$

It clearly appears that the role of the Glan-Taylor prism consists in avoiding the influence of the grating on the polarization rate measurements. However, the polarization effect of the grating does not perturb the measurements of Γ only if the polarization direction of the Glan-Taylor prism is correctly adjusted at 45° to the ion beam direction. This condition is verified beforehand by analyzing the light of a mercury lamp purely polarized by a Wollaston prism either parallel or perpendicular to the ion beam direction. With such a device, one can select the polarization direction of the Glan-Taylor prism which is either parallel or perpendicular to the ion beam direction simply by trying to obtain the maximum and the minimum of transmission, respectively. When this adjustment is done, one has only to fix mechanically its polarization direction at 45° to the ion beam direction. A drastic check of its correct orientation can be found in the fact that Γ must be the same for a given wavelength in any diffraction order of the grating. In particular, we have verified that an unpolarized light is indeed detected unpolarized.

The accuracy of the determination of Γ depends on the quality of the optical device but also on the error in the reading of the recorded signals $i_{\parallel}-i_{\min}$ and $i_{\perp}-i_{\min}$. For a well-prepared optical device, this latter source of error is preponderant and will be considered only hereafter.

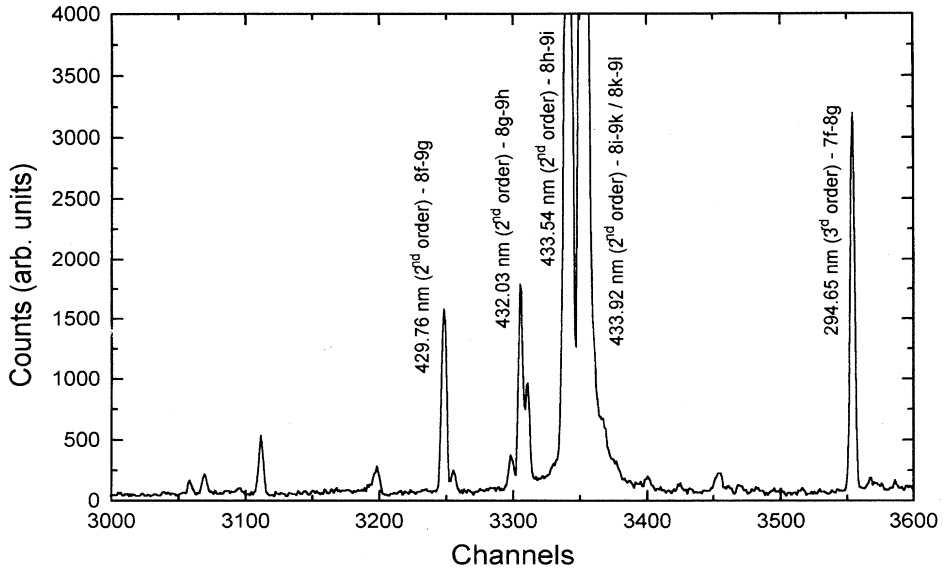

FIG. 1. Part of the 120-keV Ar^{8+}-Li spectrum in the range 420–445 nm in the second order.

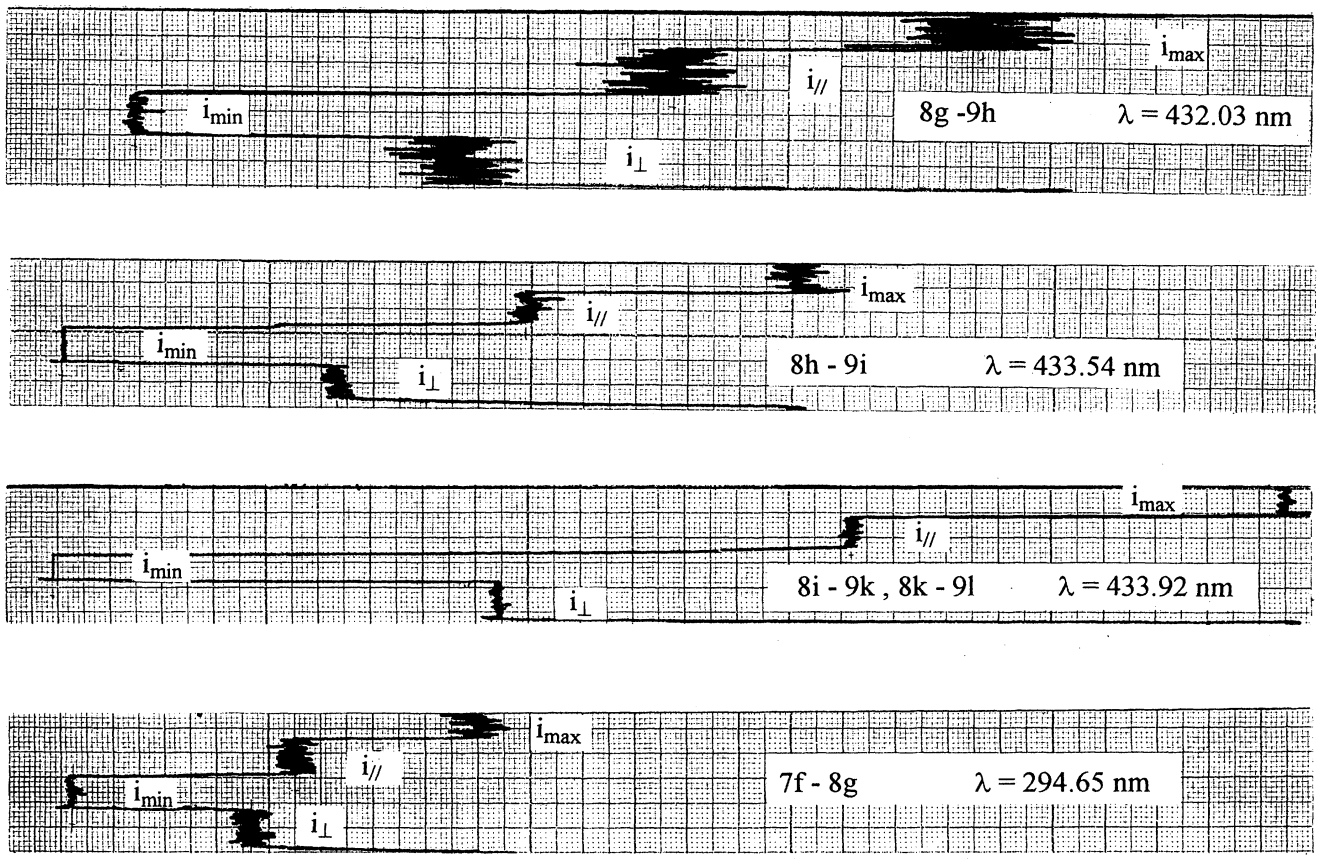

FIG. 2. Recordings of the intensities $i_{\parallel}$, $i_{\perp}$, $i_{\min}$, and $i_{\max}$ of the $7f$-$8g$, $8g$-$9h$, $8h$-$9i$ and $8i$-$9k$, $8k$-$9l$ lines observed during Ar^{8+}-Li collisions at 80 keV.

III. EXPERIMENTAL RESULTS AND INTERPRETATION

The emission spectra resulting from the collisions of Ar^{8+} ions on lithium atoms at intermediate velocities in the 200–600 nm wavelength range and their analysis have already been presented earlier by Jacquet *et al.* in [1]. These spectra mainly include lines corresponding to $n'l'$-nl transitions with $\Delta n = n - n' = 1$ and 2. These lines result from the decay of the Ar^{7+} excited ions produced by the single-electron-capture process which preferentially populates the $n = 8$ and 9 configurations. As an example, a part of the Ar^{8+}-Li spectrum recorded by Jacquet *et al.* [1] for a projectile energy of 120 keV is presented in Fig. 1.

The polarization rate of each line observed for a collision energy of 80 keV is deduced from the measurements of the intensities $i_{\parallel}$, $i_{\perp}$, $i_{\min}$, and $i_{\max}$ corresponding to the different orientations of the dichroic polarizer, as explained in Sec. II. To account for the experimental data, the recordings related to the lines observed in Fig. 1 are shown in Fig. 2. For clarity, only one measurement of each intensity is reported here. In fact, several measurements of $i_{\parallel}$, $i_{\perp}$, $i_{\min}$, and $i_{\max}$ were performed for each line in order to minimize the statistical errors. The experimental polarization rate was then averaged over the measurements. The measured polarization rates corresponding to $7l$-$8l'$ and $8l$-$9l'$ transitions are given, for a collision energy of 80 keV in Tables I and II, respectively.

TABLE I. Experimental and theoretical polarization rates of the emission lines corresponding to $7l$-$8l'$ transitions resulting from single-electron capture following 80-keV Ar^{8+}-Li collisions. (1) Experimental polarization rates. (2) Polarization rates calculated assuming only $m_l = 0$ sublevels populated. (3) Polarization rates calculated by using the m_l distributions obtained with the CTMC method.

Transition	Wavelength (nm)	Γ_{expt} (%) (1)	$\Gamma_{m=0}$ (%) (2)	Γ_{CTMC} (%) (3)
$7p_{1/2}$-$8s_{1/2}$	300.66	-2.3 ± 5.0	0	0
$7p_{3/2}$-$8s_{1/2}$	302.18	-0.2 ± 3.0	0	0
$7d_{5/2}$-$8p_{3/2}$	362.00	1.8 ± 2.4	14.3	-1.5
$7d_{3/2}$-$8p_{1/2}$	363.31	-2.6 ± 2.6	0	0
$7f$-$8d$	319.87	-1.3 ± 5.0	20.0	0.0
$7f$-$8g$	294.65	11.7 ± 2.6	45.5	16.5
$7g$-$8h$	297.18	17.3 ± 1.5	42.9	15.2
$7h$-$8i$	297.46	25.0 ± 1.8	41.2	19.9
$7i$-$8k$			40.0	25.6

TABLE II. Experimental and theoretical polarization rates of the emission lines corresponding to $8l$-$9l'$ transitions resulting from single-electron capture following 80-keV Ar^{8+}-Li collisions. (1) Experimental polarization rates. (2) Polarization rates calculated assuming only $m_l=0$ sublevels populated. (3) Polarization rates calculated by using the m_l distributions obtained with the CTMC method.

Transition	Wavelength (nm)	Γ_{expt} (%) (1)	$\Gamma_{m=0}$ (%) (2)	Γ_{CTMC} (%) (3)
$8p_{1/2}$-$9s_{1/2}$	448.23	1.7±4.6	0	0
$8p_{3/2}$-$9s_{1/2}$	450.47	−1.6±2.6	0	0
$8f$-$9g$	429.76	22.1±4.6	45.5	27.3
$8g$-$9h$	432.03	26.4±2.4	42.9	28.1
$8h$-$9i$	433.54	25.1±1.4	41.2	29.5
$8i$-$9k$	433.92	28.2±2.8	40.0	31.7
$8k$-$9l$			39.1	32.5

Two characteristic features are observed.

(i) The lines emitted from states of large l values are strongly polarized *along the ion beam direction*. The polarization rates reach values up to about 30% for yrast transitions.

(ii) The transitions between states of low l values are found to be weakly polarized or unpolarized. However, some caution has to be taken in regard to the relative uncertainties which are larger than 100% in those cases. Let us note that np-$n's$ transitions are not polarized. Indeed, the projection of s states along the beam axis is null. This shows that the optical device is well oriented.

For a further analysis, the polarization rates were related to the populations of the magnetic m_l sublevels. The quantization axis is determined by the ion beam direction. Let us consider the transition from the $|\gamma J\rangle$ level to the $|\gamma' J'\rangle$ level. The intensities $I_\parallel$ and $I_\perp$ are linked to the σ_{JM_J} Zeeman sublevel populations in the following way.

$$I_\parallel \propto \sum_{\substack{M_J,M'_{J'} \\ M_J=M'_{J'}}} \sigma_{JM_J} \begin{pmatrix} J & 1 & J' \\ -M_J & 0 & M'_{J'} \end{pmatrix}^2, \tag{5}$$

$$I_\perp \propto \sum_{\substack{M_J,M'_{J'} \\ M_J=M'_{J'}+1}} \sigma_{JM_J} \begin{pmatrix} J & 1 & J' \\ -M_J & 1 & M'_{J'} \end{pmatrix}^2 = \sum_{\substack{M_J,M'_{J'} \\ M_J=M'_{J'}-1}} \sigma_{JM_J} \begin{pmatrix} J & 1 & J' \\ -M_J & -1 & M'_{J'} \end{pmatrix}^2. \tag{6}$$

Our interest is focused on the populations of the $|\gamma l s m_l m_s\rangle$ substates which are related to the σ_{JM_J} by the following expression:

TABLE III. Relative populations of $Ar^{7+}(8l)$ Zeeman substates computed by using the CTMC method for 80-keV Ar^{8+}-Li collisions.

	m							
Substate	0	±1	±2	±3	±4	±5	±6	±7
$8s$	100%							
$8p$	26.4%	36.8%						
$8d$	18.8%	20.8%	19.8%					
$8f$	17.0%	14.1%	16.1%	11.3%				
$8g$	16.6%	14.6%	13.5%	8.8%	4.8%			
$8h$	11.8%	12.7%	11.6%	9.5%	7.2%	3.1%		
$8i$	12.2%	12.9%	10.9%	9.0%	6.2%	2.4%	2.5%	
$8k$	13.6%	13.4%	12.6%	8.1%	4.4%	2.2%	1.5%	1.0%

$$\sigma_{JM_J} = \sum_{\substack{m_l,m_s \\ m_l+m_s=M_J}} |\langle \gamma l s m_l m_s | JM_J\rangle|^2 \sigma_{m_l}\sigma_{m_s}. \tag{7}$$

The target is not prepared in a magnetic aligned state; i.e., $\sigma_{m_s}=\sigma_{-m_s}$. Moreover, the ion beam is a rotation axis for the experience, so $\sigma_{m_l}=\sigma_{-m_l}=\sigma_{|m_l|}$.

When the wavelengths of the lines corresponding to the three $\gamma J \rightarrow \gamma' J'$ transitions of the $nl \rightarrow n'l'$ transition are close, we have to evaluate the polarization rate of the $|\gamma l s m_l m_s\rangle \rightarrow |\gamma' l' s m'_l, m'_s\rangle$ transition. Following Fano and Macek [17], we have chosen to calculate the alignment parameter:

$$A(l) = -p(0) + 2\sum_{m_l=1}^{l} \frac{3m_l^2 - l(l+1)}{l(l+1)} p(|m_l|) \tag{8}$$

with

$$p(0) = \frac{\sigma_0}{\sigma_0 + 2\sum_{m_l=1}^{l} \sigma_{|m_l|}}, \quad p(|m_l|) = \frac{\sigma_{|m_l|}}{\sigma_0 + 2\sum_{m_l=1}^{l} \sigma_{|m_l|}}. \tag{9}$$

For the transition $|\gamma l\rangle \rightarrow |\gamma' l'\rangle$, the polarization rate is then

$$\Gamma(l,l') = \frac{I_\parallel - I_\perp}{I_\parallel + I_\perp} = \frac{3h(l,l')A(l)}{4 + h(l,l')A(l)} \tag{10}$$

with

$$h(l,l') = (-1)^{l-l'} \begin{Bmatrix} l & l & 2 \\ 1 & 1 & l' \end{Bmatrix} \begin{Bmatrix} l & l & 2 \\ 1 & 1 & l \end{Bmatrix}^{-1}. \tag{11}$$

However, it is obvious that the measurement of the polarization rate of a given transition cannot lead to the experimental determination of the Zeeman sublevel populations for a principal reason: as soon as $l>2$, the number of Zeeman sublevel populations to compute becomes larger than the number of equations to solve.

In fact, we have adopted the following position. In a first approach, we have assumed that the projection of the angular momentum along the quantization axis was conserved during

TABLE IV. Relative populations of $Ar^{7+}(9l)$ Zeeman substates computed by using the CTMC method for 80-keV Ar^{8+}-Li collisions.

	m								
Substate	0	±1	±2	±3	±4	±5	±6	±7	±8
$9s$	100%								
$9p$	39.8%	30.1%							
$9d$	31.2%	25.1%	9.3%						
$9f$	25.6%	21.7%	11.6%	3.9%					
$9g$	20.2%	19.8%	12.5%	6.4%	1.2%				
$9h$	18.4%	17.4%	13.4%	6.7%	2.8%	0.5%			
$9i$	16.8%	16.8%	13.8%	7.1%	2.2%	1.1%	0.6%		
$9k$	18.0%	16.6%	13.4%	6.8%	2.4%	0.9%	0.6%	0.3%	
$9l$	17.2%	17.7%	12.7%	6.5%	2.3%	1.2%	0.6%	0.3%	0.1%

the collision. In such an assumption and since the collisional system is formed of an Ar^{8+} ion and a Li atom in their ground states, only $m_l=0$ substates were expected to be produced during the capture process. In that case, the corresponding polarization rates are easily computed for any transition. The results obtained in that manner are denoted $\Gamma_{m=0}$ and are reported in Tables I and II. It is then clear that the assumption of the population of only the $m_l=0$ sublevels is not sufficient to explain the measured polarization rates which are found to be smaller except the np-$n's$ transitions which are never polarized.

In a second approach, we have used the m_l distributions calculated by the classical trajectory Monte Carlo method (CTMC). Details on the CTMC calculations and more specifically on the binning procedure of the classical quantities (for every trajectory ending to the electron-capture process) to the final quantum numbers n and l have already been published [1,2,9]. In this work, as also in Ref. [10], we have determined the final magnetic quantum number m_l corresponding to a sublevel l from the projection L_c^Z along the projectile initial velocity (taken as the quantization axis) of the electron classical angular-momentum vector $\vec{L}_c$, relative to the projectile, and from the condition [18]

$$\frac{2m_l-1}{2l+1} \leqslant \frac{L_c^Z}{L_c} < \frac{2m_l+1}{2l+1} . \tag{12}$$

This condition, which produces the correct quantal distribution of m_l within the nl sublevel, is a natural extension of the ones previously used in Refs. [9,19].

The CTMC results are reported in Tables III and IV. It is worth noting that the CTMC method predicts a nonstatistical m_l distribution for each nl configuration presented here, with low m_l values preferentially populated. In general, $m_l=0$, ± 1 but also $m_l=\pm 2$ are the most populated substates, while the population of the m_l substates with $|m_l|\geqslant 3$ decreases with increasing $|m_l|$ values. In the case of the most populated $n=8$ and 9 levels, the $m_l=0$, ± 1 substates tend to be nearly equally populated for the largest values of l. The statistical errors in the CTMC calculated m_l distributions within an nl sublevel, and for the most populated m_l values, are estimated to be less than 10% for both the $8l$ and $9l$ sublevels.

The polarization rates calculated using such distributions are denoted Γ_{CTMC} and are reported in Tables I and II. The results presented here have been obtained without taking into account the radiative cascade effects as it is done in Ref. [20]. A specific calculation of such effects has been done for the $7i$-$8k$ transition whose polarization rate is expected to be

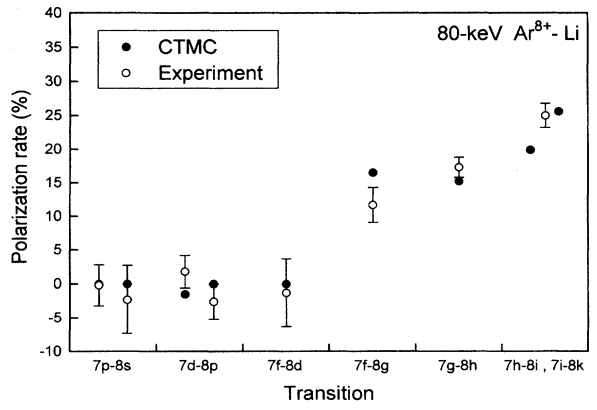

FIG. 3. Experimental and theoretical polarization rates of the emission lines corresponding to $7l$-$8l'$ transitions. For the $7p$-$8s$ and the $7d$-$8p$ transitions, respectively, the left symbols correspond to the $7p_{3/2}$-$8s_{1/2}$ and the $7d_{5/2}$-$8p_{3/2}$ transitions, and the right symbols correspond to the $7p_{1/2}$-$8s_{1/2}$ and the $7d_{3/2}$-$8p_{1/2}$ transitions.

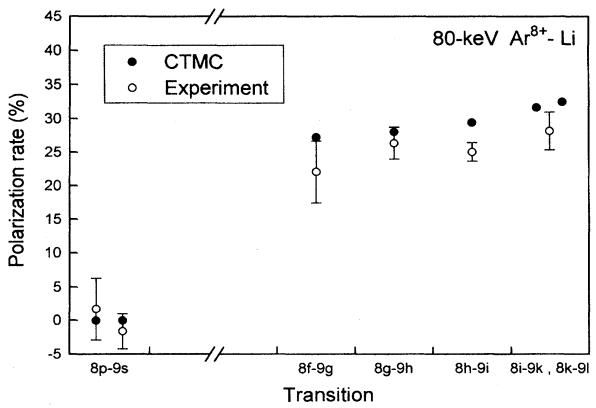

FIG. 4. Experimental and theoretical polarization rates of the emission lines corresponding to $8l$-$9l'$ transitions. For the $8p$-$9s$ transition, the left symbols correspond to the $8p_{1/2}$-$9s_{1/2}$ transition, and the right symbols correspond to the $8p_{3/2}$-$9s_{1/2}$ transition.

significantly perturbed by the $8k$-$9l$ transition. This calculation shows that the polarization rate increases from 25.6% to 28.5%. Considering the error bars, the polarization rates of the other lines should not be strongly affected by the cascades. Within the experimental uncertainties, we observe a fair agreement between the experimental polarization rates and the calculated ones (Figs. 3 and 4).

The CTMC m_l distributions are more appropriate than the $m_l=0$ distributions to explain our experimental results. The fact that the projection of the angular momentum along the quantization axis is not conserved during the collision can be explained as a consequence of postcollisional effects and more specifically as a consequence of the electric field of the residual Li^+ ion inducing rotational coupling. Such a situation is similar to that predicted by Salin [8] in the case of collision of fully stripped ions on hydrogen atoms.

IV. CONCLUSION

Summarizing, we have measured the polarization rates of Ar^{7+} emission lines resulting from single-electron transfer in Ar^{8+}-Li collisions at 80 keV. The obtained results indicate an alignment of substates of large l values, characterized by a strong polarization of the corresponding lines along the ion beam direction. These measured polarization rates are in good agreement with those determined from Zeeman sublevel distributions calculated by using the CTMC method. This agreement confirms the reliability of the CTMC calculations which predict that low m_l final sublevels ($m_l=0$, ± 1, and ± 2) are predominantly produced.

These CTMC m_l distributions are similar to the m_l distributions calculated by Salin [8] in the case of collisions of fully stripped ions on hydrogen atoms. In this case the strong alignment observed here can be interpreted as a consequence of the primary capture process itself which populates *an initial* $m_l=0$ *substate*. As a consequence, the loss of alignment which manifests itself in the population of the $m_l\neq 0$ sublevels might be due to postcollisional effects. Further theoretical and experimental efforts are, however, needed to lead to a better understanding of the single-electron-capture process. In particular, it is of interest to study the dependence of the polarization rates on the collision energy and on the electron core of the projectile.

[1] E. Jacquet, P. Boduch, M. Chantepie, M. Druetta, D. Hennecart, X. Husson, D. Lecler, R. E. Olson, J. Pascale, N. Stolterfoht, and M. Wilson, Phys. Scr. **47**, 619 (1993).

[2] E. Jacquet, J. Pascale, P. Boduch, M. Chantepie, and D. Lecler, J. Phys. B **28**, 2221 (1995).

[3] R. Abrines and I. C. Percival, Proc. Phys. Soc. **88**, 861 (1966).

[4] R. E. Olson and A. Salop, Phys. Rev. A **16**, 531 (1977).

[5] E. Jacquet, P. Boduch, M. Chantepie, M. Druetta, D. Hennecart, X. Husson, D. Lecler, F. Martin-Brunetière, R. E. Olson, J. Pascale, and M. Wilson, Phys. Scr. **49**, 154 (1994).

[6] J. Burgdörfer, Phys. Rev. A **24**, 1756 (1981).

[7] C. Harel and H. Jouin, J. Phys. B **21**, 859 (1988).

[8] A. Salin, J. Phys. (Paris) **45**, 671 (1984).

[9] J. Pascale, R. E. Olson, and C. O. Reinhold, Phys. Rev. A **42**, 5305 (1990).

[10] E. Jacquet and J. Pascale, Nucl. Instrum. Meth. Phys. Res. Sect. B **98**, 253 (1995).

[11] S. J. Czuchlewski, L. D. Ellsworth, J. A. Guffey, E. Horsdal Pedersen, E. Salzborn, and J. R. MacDonald, Phys. Lett. **51A**, 309 (1975).

[12] R. Baptist, J. J. Bonnet, G. Chauvet, J. P. Desclaux, S. Dousson, and D. Hitz, J. Phys. B **17**, L417 (1984).

[13] D. Vernhet, A. Chetioui, K. Wohrer, J. P. Rozet, P. Piquenal, D. Hitz, S. Dousson, A. Salin, and C. Stephan, Phys. Rev. A **32**, 1256 (1985).

[14] R. L. Watson, J. Palinkas, G. J. Pedrazzini, B. Bandong, C. Can, D. A. Church, and R. A. Kenefick, Phys. Rev. A **35**, 1510 (1987).

[15] P. Roncin, C. Adjouri, M. N. Gaboriaud, L. Guillemot, M. Barat, and N. Andersen, Phys. Rev. Lett. **65**, 3261 (1990).

[16] L. J. Lembo, K. Danzmann, Ch. Stoller, W. E. Meyerhof, and T. W. Hänsch, Phys. Rev. A **37**, 1141 (1988).

[17] U. Fano and J. F. Macek, Rev. Mod. Phys. **45**, 553 (1973).

[18] R. E. Olson and J. Pascale (private communication).

[19] G. A. Kohring, A. E. Wetmore, and R. E. Olson, Phys. Rev. A **28**, 2526 (1983).

[20] C. D. Lin and J. H. Macek, Phys. Rev. A **35**, 5005 (1987).